Published by IOP Publishing for SISSA

Received: *October 7, 2008*
Revised: *March 26, 2009*
Accepted: *April 10, 2009*
Published: *May 6, 2009*

Small-x single-particle distributions in jets from the coherent branching formalism

Sebastian Sapeta[a] **and Urs Achim Wiedemann**[b]

[a] *M. Smoluchowski Institute of Physics, Jagellonian University, Reymonta 4, 30-059 Cracow, Poland*
[b] *Department of Physics, CERN, Theory Division, CH-1211 Geneva 23, Switzerland*

E-mail: sapeta@th.if.uj.edu.pl, Urs.Wiedemann@cern.ch

Abstract: We calculate single parton distributions inside quark and gluon jets within the coherent branching formalism, which resums leading and next-to-leading logarithmic contributions. This formalism is at the basis of the modified leading logarithmic approximation (MLLA), and it conserves energy exactly. For a wide preasymptotic range of the evolution variable $Y = \ln[E\theta/Q_0]$, we find marked differences in the shape and norm of single parton distributions calculated in the MLLA or in the coherent branching formalism, respectively. For asymptotically large values of Y, the difference in norm persists, while differences in shape disappear. In this way, our study allows us to compare the MLLA approach, which is of particular physics interest because of its phenomenological success, to a formalism which at the same parametric accuracy implements additional physics features expected for a more complete calculation. We discuss in particular the qualitative differences between both formalisms in the limit of very small hadronization scale $Q_0 \to \Lambda_{\mathrm{QCD}}$, in which the MLLA formalism approaches a limiting spectrum. We identify why the coherent branching formalism does not allow for a limiting spectrum and we comment on the implications for hadronization pictures based on local parton hadron duality.

Keywords: Jets, QCD

ArXiv ePrint: 0809.4251

doi:10.1088/1126-6708/2009/05/023

JHEP05(2009)023

Contents

1 Introduction

Since the early days of QCD, it has been known that destructive interference between soft gluon emissions within a jet suppresses hadron production at small values of the momentum fraction $x = p_h/E$. For inclusive single-parton distributions, this is seen already in the double logarithmic approximation (DLA), which predicts a hump-backed plateau [1]. However, if one considers the kinematic regime of sufficiently small momentum fractions x, and sufficiently large jet energies E, where $\ln[1/x] \sim \ln[E/Q_0] \sim \mathcal{O}\left(1/\sqrt{\alpha_s}\right)$, then corrections to the asymptotic DLA result are of relative order $\sqrt{\alpha_s}$ for the peak position of the hump-backed plateau [1–3]. These corrections remain sizable up to the highest experimentally accessible jet energies. The coherent parton branching formalism [4, 5] leads to evolution equations for the inclusive single- and multi-parton intra-jet distributions, which contain the complete set of next-to-leading $\mathcal{O}(\sqrt{\alpha_s})$ corrections, as well as a subset of higher order corrections. The modified leading logarithmic approach (MLLA) [5, 6] to inclusive parton distributions, which is at the basis of many phenomenological comparisons, can be obtained from these evolution equations after further approximations.[1]

One may ask whether the evolution equations of the coherent branching formalism contain more physics than MLLA. This idea is not supported by parametric considerations,

[1] The evolution equations of the coherent branching formalism are defined in (2.3) below. Throughout this work, we follow common practice by using the label 'MLLA' for solutions of the equations (2.16) and (2.17).

JHEP05(2009)023

since both MLLA and the original evolution equations are complete up to the same order in $\sqrt{\alpha_s}$. However, the idea is supported by kinematic considerations, since the original evolution equations conserve energy exactly, while MLLA does not. This has motivated in recent years several works which aim at going beyond MLLA. In particular, in an approach referred to as NMLLA [7–9], one keeps all terms of the original evolution equations, which are one order $\mathcal{O}(\sqrt{\alpha_s})$ higher than the MLLA accuracy. In the same manner also a subset of $\mathcal{O}(\alpha_s)$ corrections to MLLA have been determined [10, 11]. On the other hand, one may solve the original evolution equations numerically without any further approximation. So far, this has been done for fully integrated partonic jet multiplicities only [12, 13]. The main result of the present work is to solve these original evolution equations for the inclusive single-parton distributions, to compare the numerical results to those of MLLA, and to identify the analytical origin and numerical consequences of the differences between both.

It has been emphasized repeatedly that the QCD prediction for the hump-backed plateau of the single inclusive distribution remains unaffected by the non-perturbative hadronization process as long as hadronization is sufficiently local so that it does not alter significantly the shapes of partonic momentum distributions. In particular, the phenomenologically successful comparison of the (rescaled) partonic MLLA prediction with inclusive hadronic distributions supports a local parton-hadron duality (LPHD) underlying the hadronization mechanism [14, 15]. This success of MLLA supplemented by LPHD is based on the so-called MLLA limiting spectrum, which is obtained by continuing the perturbative evolution down to $Q_0 = \Lambda_{\mathrm{QCD}}$. On the other hand, other phenomenologically successful approaches, e.g. those employed in Monte Carlo event generators, stop perturbative evolution at a significantly larger scale $Q_0 \sim \mathcal{O}(1\,\mathrm{GeV})$. The corresponding hadronization models, such as the Lund string fragmentation or cluster hadronization lead to a significant further softening of single-inclusive distributions during hadronization [16–18]. This raises the question to what extent extrapolating the perturbative evolution into the nominally non-perturbative regime between Λ_{QCD} and $\mathcal{O}(1\,\mathrm{GeV})$ can account for the dynamics of hadronization. We note that the perturbative evolution implemented in modern MC event generators has the same parametric accuracy as MLLA and the coherent branching formalism, and it conserves energy exactly as does the coherent branching formalism.[2] Beyond obtaining an additional test for the robustness of the physics conclusions drawn from the phenomenologically successful MLLA approach, we thus expect to add to our picture of the hadronization process by studying analytically and numerically for Q_0 close to Λ_{QCD} the differences between MLLA and the exact solution in the coherent branching formalism.

The paper is organized as follows. In section 2, we introduce the equations of the coherent branching formalism [4, 5], we discuss in detail their relation to the MLLA approach in section 2.2, and we describe shortly how we solve these evolution equations. Section 3 presents a numerical comparison of both formalisms. In particular, we focus in section 3.3 on the qualitative differences between both formalisms in the limit $Q_0 \to \Lambda_{\mathrm{QCD}}$, and we isolate the analytical origin of this difference. We then discuss in section 3.4, to what extent

[2]For the present study, the use of the coherent branching formalism is advantageous, since the approximations leading from the coherent branching formalism to MLLA can be stated analytically and can be tested separately.

JHEP05(2009)023

for hadronization scales Q_0 close to $\Lambda_{\rm QCD}$, characteristic differences between the coherent branching formalism and MLLA remain, if one allows for the freedom of adapting the norm and hadronization scale independently in both approaches. This amounts to studying to what extent the coherent branching formalism supplemented with LPHD at very low scale Q_0 can be brought into agreement with the MLLA limiting spectrum, which has been phenomenologically successful. The physical origin of several characteristic features of the coherent branching formalism, which are not as prominent in the MLLA approach, can be understood by studying separately the distributions of quarks and gluons in a quark or a gluon jet. The corresponding results are discussed shortly in section 4. Our conclusions are summarized in section 5.

2 Evolution equations for single parton distributions at small x

We want to calculate the single distributions $D_q(x,Y)$ and $D_g(x,Y)$ of partons in a quark or gluon jet, respectively. Here, $x = p/E$ is the jet momentum fraction of partons, and the variable

$$Y = \ln \frac{E\theta}{Q_0} \tag{2.1}$$

is written in terms of the sufficiently small jet opening angle θ, and the hadronic scale Q_0. We denote the logarithm of the momentum fraction by

$$l = \ln \frac{1}{x}\,. \tag{2.2}$$

In the coherent parton branching formalism, the evolution equations for these distributions are given by [4, 5]

$$\begin{aligned}
\partial_Y D_q(x,Y) &= \frac{1}{2}\int_{z_-}^{z_+} dz\, \frac{\alpha_s(k_\perp^2)}{\pi} \\
&\quad \times\Big\{ P_{qq}(z)\left[D_q\left(\frac{x}{z},Y+\ln z\right)+D_g\left(\frac{x}{1-z},Y+\ln(1-z)\right)-D_q(x,Y)\right] \\
&\quad + P_{gq}(z)\left[D_g\left(\frac{x}{z},Y+\ln z\right)+D_q\left(\frac{x}{1-z},Y+\ln(1-z)\right)-D_q(x,Y)\right]\Big\}, \\
\partial_Y D_g(x,Y) &= \frac{1}{2}\int_{z_-}^{z_+} dz\, \frac{\alpha_s(k_\perp^2)}{\pi} \\
&\quad \times\Big\{ P_{gg}(z)\left[D_g\left(\frac{x}{z},Y+\ln z\right)+D_g\left(\frac{x}{1-z},Y+\ln(1-z)\right)-D_g(x,Y)\right] \\
&\quad + 2n_f\, P_{qg}(z)\left[D_q\left(\frac{x}{z},Y+\ln z\right)+D_q\left(\frac{x}{1-z},Y+\ln(1-z)\right)-D_g(x,Y)\right]\Big\},
\end{aligned} \tag{2.3}$$

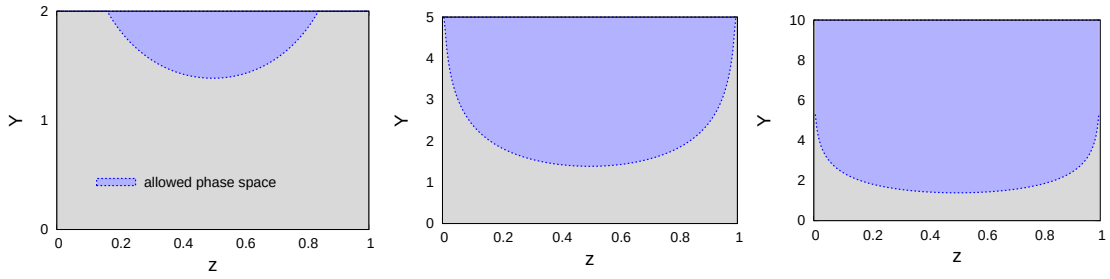

Figure 1. The range (2.6) of z-values, which are kinematically allowed in the evolution of the single-parton distributions $D_q(x,Y)$, $D_g(x,Y)$ up to $Y=2$ (left), $Y=5$ (middle), $Y=10$ (right).

with the unregularized splitting functions

$$\begin{aligned} P_{qq}(z) &= C_F \frac{1+z^2}{1-z}, \\ P_{gg}(z) &= 2C_A \left(\frac{1-z}{z} + \frac{z}{1-z} + z(1-z) \right), \\ P_{qg}(z) &= T_R \left(z^2 + (1-z)^2 \right), \qquad T_R = \frac{1}{2}, \\ P_{gq}(z) &= C_F \frac{1+(1-z)^2}{z}. \end{aligned} \tag{2.4}$$

To calculate jet multiplicity distributions with next-to-leading logarithmic accuracy, one can use a DGLAP chain of $1 \to 2$ parton branchings which follows an exact angular ordering prescription (in contrast to the strong angular ordering prescription in DLA) and in which the coupling constant depends on $k_\perp^2$ at each vertex. In the set of evolution equations (2.3) the angular ordering is implemented by the choice of the arguments $(Y + \ln z)$ and $(Y + \ln(1-z))$ of the parton distributions and also the $k_\perp$ prescription is applied for the coupling [4].

The limits z_-, z_+ on the z-integral in (2.3) are set by the requirement that the transverse momentum $k_\perp$ is sufficiently large for perturbative evolution to be valid. That means, $k_\perp$ is larger than a hadronic scale Q_0

$$k_\perp \approx z(1-z)E\theta \geq Q_0 \quad \Rightarrow \quad Y + \ln z + \ln(1-z) \geq 0. \tag{2.5}$$

For $Y < \ln 4$, this inequality is not satisfied for any real z, so evolution occurs only for $Y > \ln 4$, where the inequality is fulfilled for

$$z_- \equiv \frac{1}{2}\Big(1 - \sqrt{1-4e^{-Y}}\,\Big) < z < z_+ \equiv \frac{1}{2}\Big(1 + \sqrt{1-4e^{-Y}}\,\Big). \tag{2.6}$$

This kinematical regime is depicted in figure 1. One can check that if (2.6) is satisfied, then the arguments $(Y + \ln z)$ and $(Y + \ln(1-z))$ of the functions D_q and D_g in (2.3) cannot

JHEP05(2009)023

be negative. The coupling constant can be written as

$$\alpha_s(k_\perp^2) = \frac{\pi}{2N_c\,\beta}\,\frac{1}{Y+\ln z+\ln(1-z)+\lambda}, \quad \beta = \frac{1}{4N_c}\left(\frac{11}{3}N_c - \frac{4}{3}n_f T_R\right), \quad \lambda = \ln\frac{Q_0}{\Lambda_{\rm QCD}}. \tag{2.7}$$

2.1 Initial conditions and ansatz for solution

A parton shower in the real world is pictured often as a quark or a gluon produced initially with high energy and virtuality and evolving perturbatively from large Y to a small hadronic scale Y_0. Evolution occurs by emitting partons at smaller and smaller angles, till a minimal angle θ_0 is reached, at which non-perturbative hadronic effects set in. The numerical solution of the evolution equations (2.3) will proceed in the opposite direction, that is, the initial conditions for the solution of (2.3) are set at the small scale Y_0 which corresponds to the final partonic state of the physical process. These initial conditions specify which partons are measured. For instance, consider the initial condition

$$D_q(x,Y_0) = \delta(1-x)\,, \qquad D_g(x,Y_0) = 0\,. \qquad \text{(Case I)} \tag{2.8}$$

This initial condition for the evolution equation specifies that the partons at the low scale Y_0 cannot split further and, by virtue of the choice (2.8), these partons are quarks. Starting the evolution from the initial condition (2.8), the functions $D_q(x,Y)$ and $D_g(x,Y)$ denote the single-*quark* distributions in a quark and a gluon jet, respectively. Alternatively, for the initial condition

$$D_q(x,Y_0) = 0\,, \qquad D_g(x,Y_0) = \delta(1-x)\,, \qquad \text{(Case II)} \tag{2.9}$$

the functions $D_q(x,Y)$ and $D_g(x,Y)$ denote the single-*gluon* distributions in a quark and a gluon jet, respectively. Previous studies [5–13] have focused on the distribution of *all* partons in a quark or a gluon jet. This is obtained by evolving $D_q(x,Y)$ and $D_g(x,Y)$ from the initial condition

$$D_q(x,Y_0) = \delta(1-x)\,, \qquad D_g(x,Y_0) = \delta(1-x)\,. \qquad \text{(Case III)} \tag{2.10}$$

In section 3 of this paper we present the results for the case of the initial condition (III) whereas in section 4 we consider cases (I) and (II).

The most general ansatz for the solutions of the evolution equations (2.3) reads

$$D_q(l,Y) = \Delta_q(Y)\,\delta(l) + Q(l,Y), \tag{2.11}$$

$$D_g(l,Y) = \Delta_g(Y)\,\delta(l) + G(l,Y). \tag{2.12}$$

Here, the discrete parts arise as a natural consequence of the initial conditions (2.8), (2.9) and (2.10). As we shall see later on, these functions, depending on the choice of initial condition, either equal identically zero or are to be identified with the Sudakov form factors, which denote the probability that a parton does not split in the evolution between Y_0 and Y. The continuous parts $Q(l,Y)$ and $G(l,Y)$ vanish at the initial scale $Y = Y_0$ and arise from the further evolution with (2.3).

2.2 The MLLA evolution equations

In the following sections, we shall compare the numerical solution of (2.3) to the results obtained from the MLLA evolution equations. Parametrically, the accuracy of both sets of equations differs only to next-to-next-to-leading order in $\sqrt{\alpha_s}$, and both sets of equations are incomplete at this order. We shall find that the solutions of both sets of evolution equations show characteristic differences. To understand these differences, we explain here how the MLLA evolution equations can be obtained from (2.3) by a set of approximations, which are valid for $Y\,, \ln[1/x] \sim \mathcal{O}(1/\sqrt{\alpha_s})$.

Counting derivatives ∂_Y, $\partial_{\ln x} \sim \mathcal{O}(\sqrt{\alpha_s})$, one sees that for a determination of the distributions $D_{q,g}$ up to $\mathcal{O}(\sqrt{\alpha_s})$, the right hand side of (2.3) has to be kept up to $\mathcal{O}(\alpha_s)$. This allows for the following approximations:

1. *Expand* $D_{q,g}\left(\frac{x}{1-z}, Y + \ln(1-z)\right)$ *for* $\ln(1-z) \ll 1$.
   In the MLLA approach, only the leading term $D_{q,g}\,(x, Y)$ is kept. The first correction is suppressed by one power of $\sqrt{\alpha_s}$ coming from ∂_Y or $\partial_{\ln x}$, and another power of $\sqrt{\alpha_s}$ coming from the fact that $\ln(1-z) \sim z$ for small z.

2. *Approximate the argument of* $\alpha_s\,(Y + \ln z + \ln(1-z))$ *by* $\alpha_s\,(Y + \ln z)$ *for singular terms and* $\alpha_s\,(Y)$ *for regular terms.*
   For terms in the integrand of (2.3), which multiply the singular part of the splitting functions, the integral is dominated by z-values close to 0 or 1. In these terms, one can approximate $\alpha_s\,(Y + \ln z + \ln(1-z)) \to \alpha_s\,(Y + \ln z)$ [after having changed $z \to 1-z$ in terms which are singular in $(1-z)$]. For terms multiplying the regular part of splitting functions, the dominant contribution to the integral comes from z not too far from $1/2$, so that one approximates $\alpha_s\,(Y + \ln z + \ln(1-z)) \to \alpha_s\,(Y)$.

3. *Approximate the boundaries* $z_\pm$.
   These boundaries arise from the kinematic constraint (2.5), which limits the z-integration to the support of $\Theta\,(Y + \ln z + \ln(1-z))$. Following the same logic as in approximating the argument of α_s, one replaces $\Theta\,(Y + \ln z + \ln(1-z)) \to \Theta\,(Y)$ for regular and $\Theta\,(Y + \ln z + \ln(1-z)) \to \Theta\,(Y + \ln z)$ for singular terms. However, the lower z-limit is effectively set by the requirement that x/z of $D_{q,g}$ is smaller than one.

4. *Further approximation in regular terms.*
   In the regular terms, the MLLA approach replaces $D_{q,g}\left(\frac{x}{z}, Y + \ln z\right)$ by $D_{q,g}\,(x, Y)$. This can be justified by counting ∂_Y, $\partial_{\ln x} \sim \mathcal{O}(\sqrt{\alpha_s})$ and observing that $\ln z$ does not give a parametric enhancement for $z \sim \mathcal{O}(1/2)$.

Applying these approximations to (2.3) and changing integration variables from $z \to (1-z)$ with the help of identities such as $P_{qq}(z) = P_{gq}(1-z)$, one arrives at the evolution equations [19]

$$\partial_Y D_q(x,Y) = \frac{C_F}{N_c}\left\{\int_0^1 \frac{dz}{z}\,\gamma_0^2(Y+\ln z)\,D_g\Big(\frac{x}{z}, Y+\ln z\Big) - a_{qg}\,\gamma_0^2(Y)\,D_g\,(x,Y)\right\}, \tag{2.13}$$

$$\partial_Y D_g(x,Y) = \int_0^1 \frac{dz}{z}\,\gamma_0^2(Y+\ln z)\,D_g\Big(\frac{x}{z}, Y+\ln z\Big) - a_{gq}\,\gamma_0^2(Y)\,D_q\,(x,Y) - a_{gg}\,\gamma_0^2(Y)\,D_g\,(x,Y)\,, \tag{2.14}$$

where $\gamma_0^2(Y) = 1/(\beta(Y+\lambda))$ and

$$a_{qg} = \frac{3}{4}, \qquad a_{gq} = -\frac{2}{3}\frac{n_f T_R}{N_c}, \qquad a_{gg} = \frac{1}{4N_c}\left(\frac{11}{3}N_c + \frac{4}{3}n_f T_R\right). \tag{2.15}$$

In equation (2.14), the parton distribution D_q in a quark jet appears only in a term which is multiplied by a prefactor of $\mathcal{O}(\alpha_s)$. Hence, to arrive at a closed expression for D_g, which is accurate to next-to-leading order in $\mathcal{O}(\sqrt{\alpha_s})$, it is sufficient to use the leading-order DLA relation

$$D_q(l,Y) = \frac{C_F}{N_c} D_g(l,Y)\,, \tag{2.16}$$

and one obtains from (2.14)

$$\partial_Y D_g(x,Y) = \int_0^1 \frac{dz}{z}\,\gamma_0^2(Y+\ln z)\,D_g\Big(\frac{x}{z}, Y+\ln z\Big) - a_1\,\gamma_0^2(Y)\,D_g\,(x,Y)\,, \tag{2.17}$$

where

$$a_1 = a_{gg} + \frac{C_F}{N_c}a_{gq} = \frac{1}{4N_c}\left[\frac{11}{3}N_c + \frac{4}{3}n_f T_R\left(1 - \frac{2C_F}{N_c}\right)\right]. \tag{2.18}$$

Eq. (2.17) is referred to as MLLA evolution equation [1, 5]. In phenomenological applications of the MLLA equation, the parton distribution in a quark jet is then commonly determined with the help of (2.16). Compared to the DLA approximation, the MLLA equation shows mainly two improvements: the coupling constant is running and the negative term $\propto -\gamma_0^2(Y)G\,(x,Y)$ on the right hand side of eq. (2.17) accounts for recoil effects which lead to a softening of the spectra as compared to DLA.

While the MLLA evolution equation (2.17) and the evolution equation (2.3) in the coherent branching formalism are complete to the same order in $\sqrt{\alpha_s}$, the approximations listed in points 1.-4. above induce characteristic qualitative changes to the results of these evolution equations. In particular:

1. *Violation of exact energy conservation*
   The small-z approximations to the integrand of (2.3), made in the approximations 1, 3 and 4 listed above, violate exact energy conservation. The numerical manifestation of this will be discussed in the context of figure 5 below.

2. *Changing the $\lambda \to 0$-behavior*
   As noted before in studies of total jet multiplicities [12, 13], the coherent branching formalism does not allow for a limiting curve, $\lambda \to 0$. In contrast, it is a peculiar feature of the MLLA approach, that its solutions have a well-defined finite limit for $\lambda \to 0$, which is known as the "limiting spectrum" and which is at the basis of many phenomenological comparisons [1, 14, 15, 20, 21]. In section 3.3, we discuss numerical results which identify the analytical origin of this qualitative difference.

3. *The Y-dependence of the discrete part of $D_{q,g}$ changes from exponential to power-law*
   In the following, all numerical results for the MLLA evolution are obtained with the

JHEP05(2009)023

initial conditions $D_g(x,Y) = \delta(1-x)$. Using the ansatz $D_g(l,Y) = \Delta_g(Y)\,\delta(l) + G(l,Y)$ of eq. (2.12), one finds for the MLLA eq. (2.17) the discrete part

$$\Delta_{\mathrm{MLLA}}(Y) = \left(\frac{Y+\lambda}{\lambda}\right)^{-a_1/\beta} \tag{2.19}$$

and the equation for the continuous part $G(l,Y)$. This expression shows a power-law dependence, while the corresponding discrete part of the solution (2.3) decays exponentially with Y.

2.3 Evolution equations in the coherent branching formalism

In this subsection, we return to the full evolution equations (2.3) of the coherent branching formalism. We study these equations with the initial condition (2.10), which corresponds to counting both quarks and gluons in the final state. In this case the discrete parts of the distributions from eqs. (2.11), (2.12) have an interpretation of the Sudakov form factors and we denote $\Delta_q(Y) \equiv S_q(Y)$ and $\Delta_g(Y) \equiv S_g(Y)$. Inserting the ansatz (2.11), (2.12) into (2.3), we find for the Sudakov form factors

$$\partial_Y S_q(Y) = -\frac{1}{2}\int_{z_-}^{z_+} dz\,\frac{\alpha_s(k_\perp^2)}{\pi}\,\left[P_{qq}(z) + P_{gq}(z)\right] S_q(Y), \tag{2.20}$$

$$\partial_Y S_g(Y) = -\frac{1}{2}\int_{z_-}^{z_+} dz\,\frac{\alpha_s(k_\perp^2)}{\pi}\,\left[P_{gg}(z) + 2n_f P_{qg}(z)\right] S_g(Y). \tag{2.21}$$

The above equations are not coupled and can be easily solved. It follows from the integration boundaries z_-, z_+ given in (2.6), that

$$S_q(Y) = S_g(Y) = 1 \qquad \text{for } Y < \ln 4\,. \tag{2.22}$$

After exploiting the $z \leftrightarrow 1-z$ symmetry of the transverse momentum (2.5) and the integration boundaries, and with the help of the property $P_{qq}(z) = P_{gq}(1-z)$, one finds for the initial condition (2.10) and for $Y > \ln 4$

$$S_q(Y) = \exp\left\{-\frac{C_F}{2N_c\beta}\int_{\ln 4}^{Y} dY' \int_{z_-}^{z_+} \frac{dz}{Y' + \ln z(1-z) + \lambda}\,\frac{1+z^2}{1-z}\right\}, \tag{2.23}$$

$$S_g(Y) = \exp\left\{-\frac{1}{4N_c\beta}\int_{\ln 4}^{Y} dY' \int_{z_-}^{z_+} dz\,\frac{dz}{Y' + \ln z(1-z) + \lambda} \times \left[2C_A\left(\frac{1-z}{z} + \frac{z}{1-z} + z(1-z)\right) + 2n_f T_R\left(z^2 + (1-z)^2\right)\right]\right\}. \tag{2.24}$$

We have performed the double integrals in eqs. (2.23) and (2.24) numerically. Figure 2 shows the result for three values of λ. For $Y > \ln 4$, these factors decrease almost exponentially. One can show that for large Y the slope changes with Y according to

$$\frac{d\ln S_{q,g}}{dY} \simeq -c_{q,g}\,\ln\left[\frac{Y+\lambda}{\lambda}\right], \tag{2.25}$$

where $c_q = C_F/(N_c\beta)$ and $c_g = 1/\beta$.

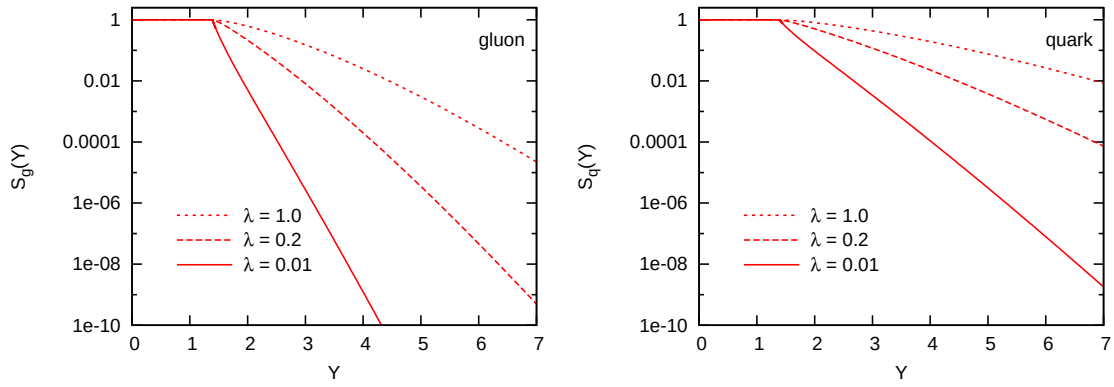

Figure 2. The Sudakov form factors (2.23) and (2.24) for three different values of λ.

The solutions $S_q(Y)$, $S_g(Y)$ enter the evolution equations for $Q(l,Y)$ and $G(l,Y)$. After changing the integration variable z to $\bar{l} = \ln(z/x)$, the equations for the continuous parts of the spectra can be written as

$$\begin{aligned}
\partial_Y Q(l,Y) &= \int_{\bar{l}_{\min}}^{\bar{l}_{\max}} d\bar{l}\,\Gamma_s(l-\bar{l},Y)\Big\{P_{qq}(l-\bar{l})\,Q(\bar{l},Y-l+\bar{l}) + P_{gq}(l-\bar{l})\,G(\bar{l},Y-l+\bar{l})\Big\} \\
&\quad + \Gamma_s(l,Y)\Big\{P_{qq}(l)\,S_q(Y-l) + P_{gq}(l)\,S_g(Y-l)\Big\} + \partial_Y \ln S_q(Y)\,Q(l,Y), \\
\partial_Y G(l,Y) &= \int_{\bar{l}_{\min}}^{\bar{l}_{\max}} d\bar{l}\,\Gamma_s(l-\bar{l},Y)\Big\{P_{gg}(l-\bar{l})\,G(\bar{l},Y-l+\bar{l}) + 2n_f P_{qg}(l-\bar{l})\,Q(\bar{l},Y-l+\bar{l})\Big\} \\
&\quad + \Gamma_s(l,Y)\Big\{P_{gg}(l)\,S_g(Y-l) + 2n_f P_{qg}(l)\,S_q(Y-l)\Big\} + \partial_Y \ln S_g(Y)\,G(l,Y),
\end{aligned} \tag{2.26}$$

where we have introduced the shorthand

$$\Gamma_s(l,Y) = \frac{1}{2N_c\beta}\,\frac{e^{-l}}{Y-l+\ln(1-e^{-l})+\lambda}. \tag{2.27}$$

The limits of integration in eq. (2.26) are

$$\bar{l}_{\min} = l - \ln\frac{2}{1-\sqrt{1-4e^{-Y}}}\,, \qquad \bar{l}_{\max} = l - \ln\frac{2}{1+\sqrt{1-4e^{-Y}}}\,. \tag{2.28}$$

We recall that the functions $G(l,Y)$ and $Q(l,Y)$ vanish when the first argument is negative. In the equations (2.26), the logarithmic derivatives $\partial_Y \ln S_{q,g}(l,Y)$ on the right hand side are formal notational shorthands, denoting the expressions (2.20), (2.21) irrespective of the initial conditions. These logarithmic derivatives decrease only logarithmically with Y, as seen from eq. (2.25). Hence, the rapid decrease of the Sudakov form factors itself does not render the corresponding terms in (2.26) negligible at large Y.

JHEP05(2009)023

3 Numerical results

We have solved numerically the evolution equations for the continuous parts of single particle distributions in quark and gluon jets in the coherent parton branching formalism (2.26) and in the MLLA approach (2.17). The solutions depend on

$$\lambda = \ln Q_0/\Lambda_{\rm QCD}\,, \tag{3.1}$$

which specifies in units of $\Lambda_{\rm QCD}$ the value of the hadronization scale Q_0 up to which the parton shower is evolved. As discussed in more detail below, the solutions for the evolution equations (2.3) can be obtained for finite values of λ, only.

In the following, we show numerical results for $\lambda = 0.01$, $\lambda = 0.2$ and $\lambda = 1.0$. The MLLA limiting spectrum is approximately $3 - 4\%$ larger in norm and similar in shape, compared to the MLLA solution for $\lambda = 0.01$. Hence, our choice for this smallest value of λ is motivated by the interest in exploring the solutions of the coherent branching formalism (2.3) for a parameter range in which the MLLA limiting spectrum is almost reached. Our choice of the largest value $\lambda = 1.0$ is motivated by the fact that parton showers implemented in Monte Carlo event generators typically end the perturbative evolution at a hadronization scale Q_0 which is significantly larger than $\Lambda_{\rm QCD}$ and for which $\lambda \sim 1$ is an order of magnitude estimate. We have chosen one value $\lambda = 0.2$ in between.

3.1 The distributions $Q(l, Y)$ and $G(l, Y)$

In figure 3, we present for $\lambda = 0.2$ results for the continuous part of the single-parton distributions inside a quark and a gluon jet, evolved from the initial condition (2.10) at $Y_0 = 0$ up to different values of Y.

We consider first the evolution for $Y < 5$. As seen in figure 3, the single inclusive distributions obtained for the evolution within the coherent branching formalism show for small Y a large yield at low values of $l \ll Y$. This effect is more pronounced for the distribution in a quark jet, than for the distribution in a gluon jet. It can be understood on general grounds from the fact that the initial conditions (2.10) for the evolution are delta-functions at $l = 0$, and that the results for small Y remember these initial conditions. Moreover, quarks are less likely to branch than gluons, and in their first branching they are likely to keep a large fraction of their energy. This tends to make the distribution in a quark jet harder than in a gluon jet, as clearly seen in figure 3. Upon further evolution to $Y = 3.3, 4.2, 5.0$, the yield of hard partons (say partons with $l < 1$) in a gluon jet decreases rapidly to a value comparable with (and for some region of l even smaller than) the results obtained in the MLLA approach. On the other hand, the yield of hard partons in a quark jet remains enhanced significantly over the yield obtained in the MLLA approach up to relatively large values of the evolution parameter Y. Also in the region around the peak of the single inclusive distributions, there are significant differences between the MLLA approach and the coherent branching formalism.

We recall that the parametric reasoning underlying the evolution equations (2.3) is valid for sufficiently large Y in the region $l \sim \mathcal{O}(Y)$ encompassing the peak. Up to $Y < 5$, the evolution shows several preasymptotic features. The right hand side of figure 3

JHEP05(2009)023

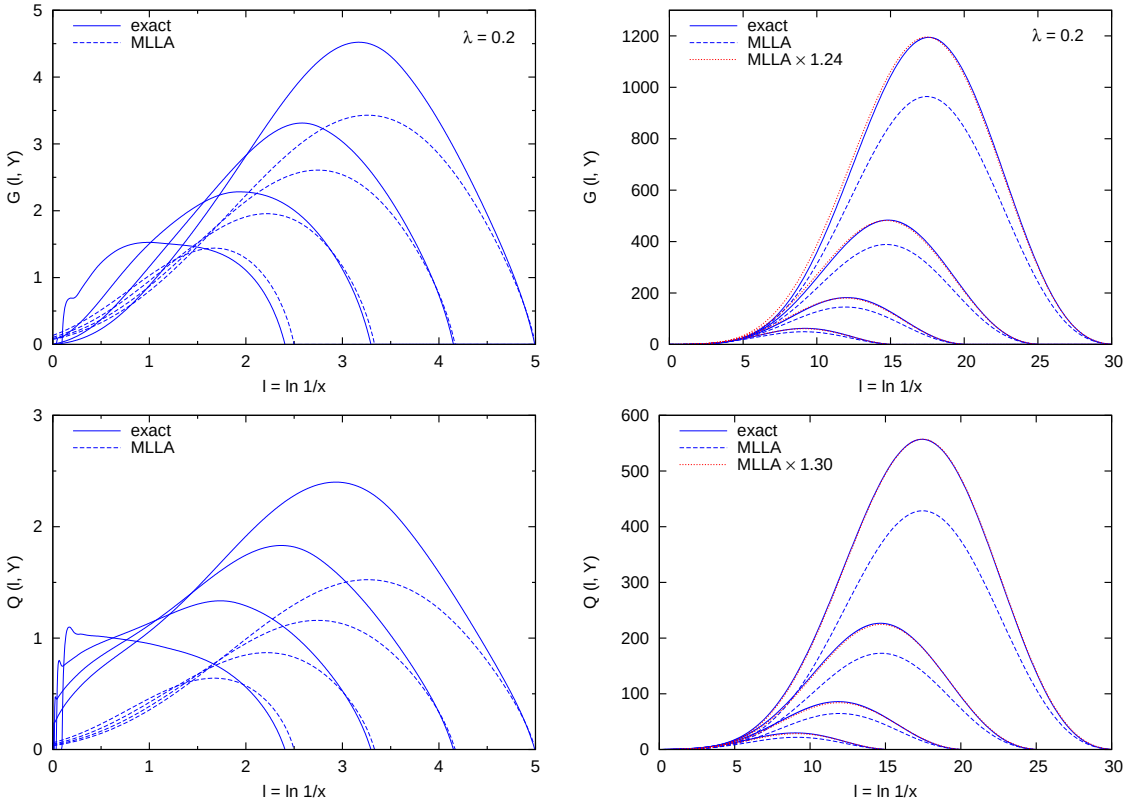

Figure 3. The continuous parts of the inclusive distribution of all partons in gluon (upper panel) and quark jet (lower panel). Results are shown for evolution in the coherent parton branching formalism (2.3), and in the MLLA approach (2.17) for $\lambda = 0.2$. Left hand side: evolution up to $Y = 2.5$, 3.3, 4.2 and 5.0. Right hand side: evolution up to $Y = 15$, 20, 25 and 30.

illustrates how these preasymptotic features become less pronounced upon further evolution in Y. The numerical results for the coherent branching formalism and the MLLA approach agree very well in shape and differ in norm by a factor of order unity which is Y-independent to good accuracy. Closer investigation shows that the factors needed to adjust the norm between both approaches differ for gluon jets (normalization factor 1.24 for $\lambda = 0.2$) and quark jets (normalization factor 1.30 for $\lambda = 0.2$). This illustrates the extent to which for sufficiently large Y, the region around the peak of the single-parton distributions lies at sufficiently large l to be calculable within the accuracy of the coherent branching formalism.

To further illustrate the slow but steady convergence in shape between the MLLA results for single-parton distributions and those of the coherent branching formalism, we have plotted in figure 4 the evolution of the peak position of these distributions as a function of Y. We see that the peak positions in both approaches differ largely for $Y \leq 5 - 7$, consistent with our earlier remarks. The value of $l_{\max}/Y$ decreases slowly with Y, but even for the largest values explored here, the position of the peak differs significantly from the DLA result $l_{\max}/Y = 1/2$.

JHEP05(2009)023

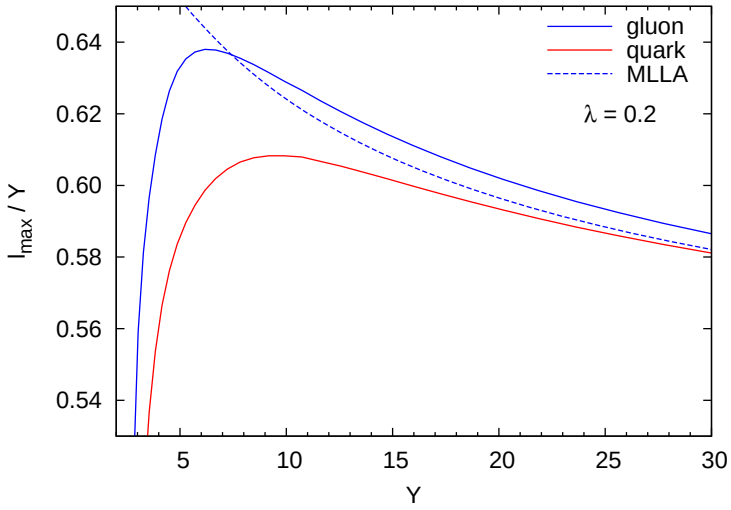

Figure 4. The evolution in Y of the peak position of the continuous parts of the inclusive parton distributions. Results are shown for all partons in a gluon jet (upper straight line) or a quark jet (lower straight line), calculated in the coherent parton branching formalism (2.3). Results are also shown for the MLLA approach (2.17) (dashed line), for which the peak positions of the distributions for quark and gluon jets coincide. All results are calculated for $\lambda = 0.2$ and the peak position $l_{\max}$ is plotted in units of Y.

3.2 Total multiplicity and energy conservation

The single-parton distributions inside quark and gluon jets can be characterized by their moments. The zeroth and first moments of the inclusive single-parton distributions are of particular interest, since they define the total parton multiplicity in a quark or gluon jet,

$$N_{q,g}(Y) = \int dl\, D_{q,g}(l, Y)\,, \tag{3.2}$$

and the total energy fraction inside a quark or gluon jet

$$\frac{1}{E} \sum_{\text{partons}} E_p(Y) = \int dx\, x D_{q,g}(x, Y)\,. \tag{3.3}$$

For an energy-conserving evolution of $D_{q,g}$, the first moment of the single-parton distribution must yield the total jet energy E, and the fraction (3.3) must equal one. As seen in the bottom panel of figure 5, this is satisfied for the coherent branching formalism. Since we know that the evolution equations (2.3) conserve energy, this is a cross check of the numerical accuracy of our solution. Energy is not conserved in the MLLA approach. We note that for sufficiently large Y, a formalism which does not conserve energy may account accurately for the functions $D_{q,g}(x, Y)$ in a wide region around the peak. This is so, since for large Y the region around the peak of $D_{q,g}$ will be at x values, which are much softer than the region of x space which contributes dominantly to (3.3).

Within the MLLA approach, one customarily uses equation (2.16) to relate the single-parton distributions in quark and gluon jets, $G(x, Y) = N_c/C_F\, Q(x, Y)$. This relation is

JHEP05(2009)023

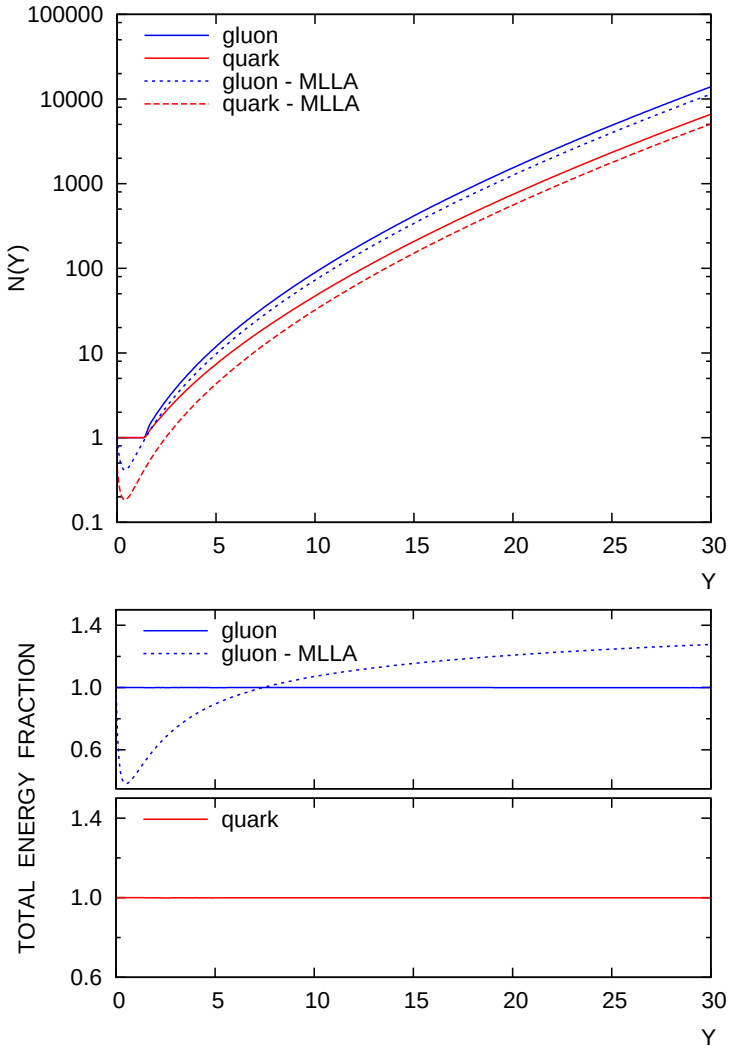

Figure 5. Upper plot: Y-dependence of the total parton multiplicity (3.2) in a quark or gluon jet, calculated in the coherent parton branching formalism (2.3) (straight lines), and in the MLLA approach (2.17) (dashed lines) for $\lambda = 0.2$. Lower plot: The ratio (3.3) of the total jet energy contained in the single parton distribution to the initial jet energy. The upper panel is for gluon jets, the lower one for quark jets, $\lambda = 0.2$.

valid to DLA accuracy and leads to the first moment (3.3) of a quark jet equal to the total energy faction of a gluon jet multiplied by 4/9. We did not include this result in figure 5, since it does not add further information.

The total parton multiplicities within a quark or a gluon jet are plotted in the upper panel of figure 5. These multiplicities satisfy evolution equations for integrated parton distributions, which are much simpler than the set of equations (2.3), and which have been studied numerically [12, 13]. We checked that we reproduce these results, if we adopt the same modifications to the coherent branching formalism (2.3). We also tested

JHEP05(2009)023

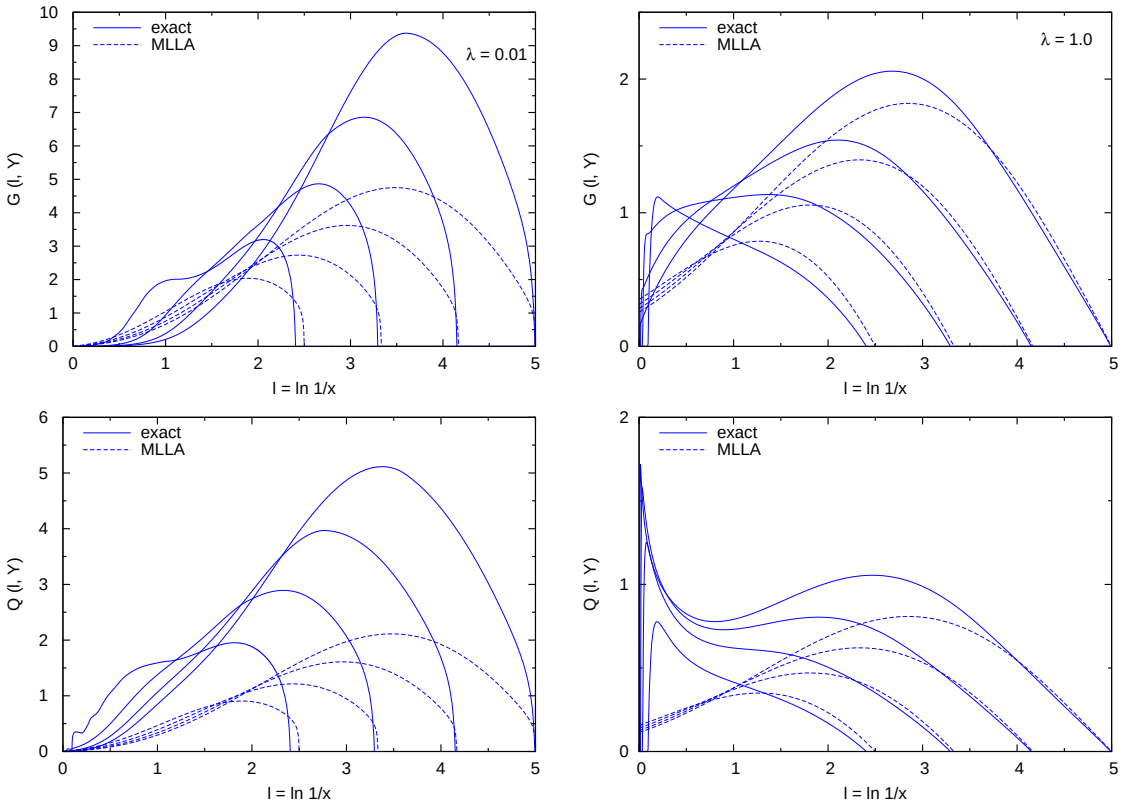

Figure 6. Same as figure 3 but for $\lambda = 0.01$ (left column) and $\lambda = 1.0$ (right column).

the numerical accuracy of our routines for $D_{q,g}(x, Y)$, by comparing the integral (3.2) to the result of the simpler evolution equations for multiplicities, and we found perfect agreement. Within MLLA, the multiplicities for the limiting case ($\lambda = 0$) and at large values of Y are known to rise like [1, 2, 7]

$$N_{\mathrm{MLLA}}(Y) \sim Y^{-a_1/(2\beta)+1/4}\, e^{2\sqrt{Y/\beta}}\,. \tag{3.4}$$

This strong rise of the multiplicity is seen in figure 5. At large Y, the rise is the same in the MLLA approach and in the coherent branching formalism. In comparison to the MLLA approach, the multiplicities obtained in the coherent branching formalism are a factor ~ 1.24 for gluon jets and a factor ~ 1.30 higher for quark jets at large Y. This is consistent with our observation in figure 3 and indicates that at large Y, the distributions obtained in both approaches can be made to coincide by an approximately Y-independent multiplicative factor.

3.3 Dependence of $Q(x, Y)$ and $G(x, Y)$ on λ

The numerical results shown in the previous subsections 3.1 and 3.2 were obtained for $\lambda = 0.2$. Here, we discuss the dependence of these results on λ. For fixed jet energy E and evolution variable Y, decreasing λ amounts to increasing Λ_{QCD}. As a consequence, a smaller value of λ is expected to lead to a more 'violent' evolution (i.e. more parton branchings)

JHEP05(2009)023

and it will thus lead to a higher jet multiplicity and a softer distribution within the same Y-interval. These general expectations are confirmed by the curves in figure 6, which show the distributions of all partons in a quark or a gluon jet for evolution over small Y-intervals up to $Y \leq 5$. In particular, for smaller λ, single parton distributions increase in multiplicity and the peak position of the distributions shifts to larger values of $\ln[1/x]$ as λ decreases.

It had been noted already in studies of total jet multiplicities [12, 13], that the coherent branching formalism does not have a finite limit $\lambda \to 0$. Our numerical studies support this observation on the level of single-inclusive parton distributions: the differences in norm between both approaches increase slowly but without bound if λ approaches zero. To identify the origin of this qualitative difference, we have tested separately the consequences of the four analytical approximations in section 2, by which the MLLA approach differs from the coherent branching formalism. We observe numerically: The solutions of equations (2.3) do not have a limiting spectrum and this does not change when these equations are modified by approximation 1 in section 2.2. But when equations (2.3) are supplemented by approximations 1 and 2 in section 2.2, a limiting spectrum arises. A limiting curve for $\lambda \to 0$ continues to exist, if one supplements (2.3) with the first three or with all four approximations listed in section 2.2. From this, we conclude that approximating the argument of the strong coupling constant $\alpha_s\left(Y + \ln z + \ln(1-z)\right) \to \alpha_s\left(Y + \ln z\right)$ in singular and $\alpha_s\left(Y + \ln z + \ln(1-z)\right) \to \alpha_s\left(Y\right)$ in regular terms on the right hand side of (2.3) is at the origin of a limiting spectrum in the MLLA approach.[3]

In general, one should not expect to obtain finite results in the limit $\lambda \to 0$, since λ regulates the Landau pole of the strong coupling constant (2.7). One may ask, however, how two approaches can show arbitrarily large numerical differences for sufficiently small values of λ, if they differ parametrically by corrections of $\mathcal{O}(\alpha_s)$ only. We note that in the limit $\lambda \to 0$, the coupling constants with approximated argument are of the form $\alpha_s\left(Y\right) \propto 1/Y$ and $\alpha_s\left(Y + \ln z\right) \propto 1/(Y + \ln z)$. This dependence is distinctly different from the assumption $Y\,, \ln[1/z] \sim \mathcal{O}\left(1/\sqrt{\alpha_s}\right)$ on which the approximations in section 2.2 are based. This illustrates that the parametric counting in powers of $\sqrt{\alpha_s}$ becomes problematic in the limit $\lambda \to 0$.

We conclude this section by discussing characteristic preasymptotic features seen in figure 6. In particular, after evolving for a few units in Y, the parton distributions for $\lambda = 1.0$ are still peaked at very large values of x, where $\ln[1/x] \ll 1$. Qualitatively, the structures at large x are due to the fact, that for small Y the phase space for evolution shown in figure 1 excludes evolution to very small values x, and the driving term of the evolution is the Sudakov form factor at $x = 1$. Upon evolution in Y, this Sudakov form factor decreases faster for the more violent evolution with $\lambda = 0.01$ than for less violent one with $\lambda = 1.0$, as can be seen from figure 2. For this reason, the parton distributions in figure 6, which were calculated with $\lambda = 0.01$, decrease under evolution in Y much faster in the region of larger x, than distributions evolved with larger values of λ. The

[3] We note that the limiting curve obtained from supplementing (2.3) with approximations 1 and 2 only differs in norm and shape from the MLLA limiting spectrum. In particular, the interplay between the argument of α_s and the integration boundaries (see approximation 3 in section 2.2) in different terms of the evolution equation is important for quantitative aspects of the solution.

JHEP05(2009)023

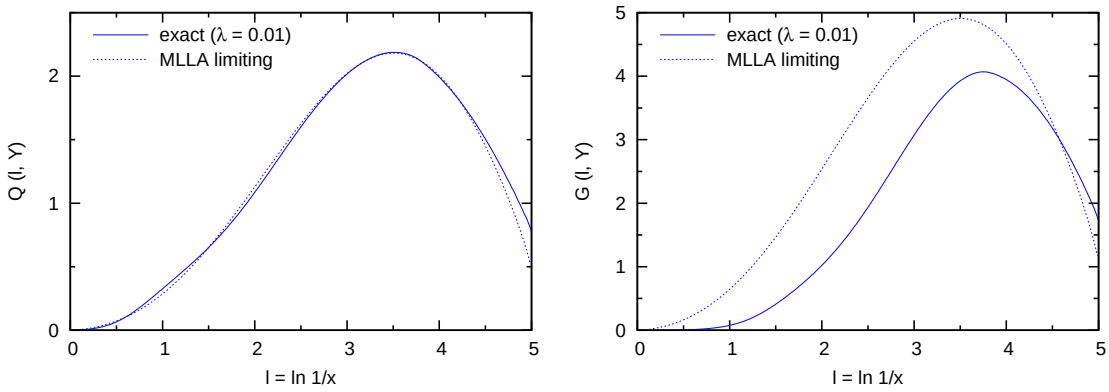

Figure 7. The continuous parts of single parton distributions. Dotted lines: the MLLA limiting fragmentation for $Y = 5.0$. Solid lines: results for the coherent branching formalism with a choice of $\lambda = 0.01$, $Y = 5.2$ and norm adjusted to 0.405 such that the distributions in quark jets almost match.

same qualitative features (though quantitatively less pronounced) are found in the MLLA approach, where for small Y the continuous part of the single parton distribution differs significantly from zero at large x, in particular for the case $\lambda = 1.0$ of a less violent evolution.

For $\lambda = 0.01$ and $\lambda = 1.0$, we have calculated the single-parton distributions inside quark and gluon jets for evolution up to $Y = 30$ (results not shown). In this asymptotic regime, similarly to the case $\lambda = 0.2$, the results obtained from the coherent branching formalism and the MLLA approach can be made to coincide by a simple adjustment of the norm. For $\lambda = 1.0$, the MLLA results are at large values of Y a factor 1.11 smaller for gluon jets and a factor 1.16 smaller for quark jets. For $\lambda = 0.01$ the corresponding factors are 1.72 for gluon jets and 1.80 for quark jets.

3.4 Matching MLLA to the coherent branching formalism

As shown in figures 3 and 6, single parton distributions calculated in the MLLA approach differ for $Y \leq 5$ both in norm and in shape from those calculated in the coherent branching formalism. Besides the normalization, the spectra depend on two additional parameters, namely Q_0 and Λ_{QCD} or equivalently Y and λ. Since the MLLA limiting fragmentation function is at the basis of many phenomenologically successful comparisons, we ask here to what extent a variation of the three parameters is sufficient to make results from the coherent branching formalism coincide with a given result of the limiting fragmentation function ($\lambda \to 0$) obtained in the MLLA approach.

Figure 7 shows an example of the extent to which this is possible. Adjusting the norm, the evolution time Y, and the value of λ, the single-parton distributions in a quark jet can be made to coincide almost for both formalisms at $Y = 5$. More generally, we find that the peak position of the single-parton distributions in either a quark or a gluon jet can always be adjusted to agree between both approaches by varying Y and λ in the coherent branching formalism. The total yield can then be adjusted by the norm. In general, small values $\lambda \ll 1$ are needed, for which the preasymptotic effects seen in figure 3 and 6 disappear rapidly with increasing Y.

JHEP05(2009)023

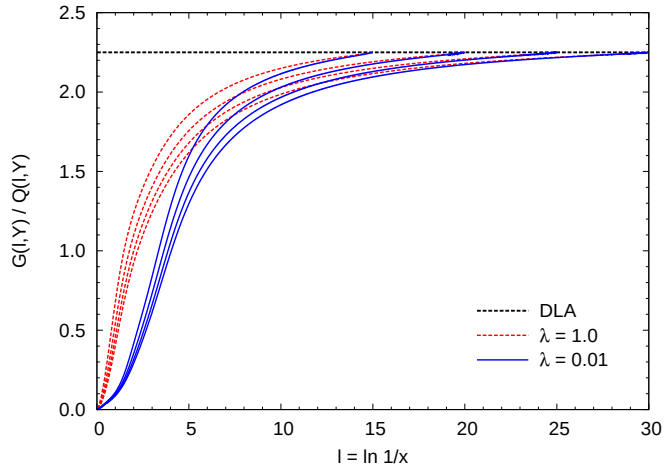

Figure 8. The ratio $G(l,Y)/Q(l,Y)$ in the coherent branching formalism for two different values of λ and evolution up to different $Y = 15$, 20, 25 and 30, from top to bottom. By construction, MLLA results assume the DLA relation (2.16).

On the other hand, it is not possible for $Y \sim 5$ and with the same choice of λ to get results of both formalisms to almost coincide for the distributions in both quark and gluon jets . This is illustrated by the example given in figure 7, where marked differences in norm and shape persist between the distributions in gluon jets, once the distributions in quark jets have been adjusted. In particular, an independent adjustment of the norm of $G(l,Y)$ is not sufficient to remove these differences. Also, we have tested (results not shown) that these differences persist if one modifies the standard MLLA procedure by including $\mathcal{O}(\sqrt{\alpha_s})$-corrections to the DLA expression (2.16) [1], which relates G and Q.

To explain why an adjustment of Y and λ cannot yield a good agreement for both distributions Q and G, calculated in MLLA and the coherent branching formalism respectively, we point to the ratio of single-parton distributions of a gluon and a quark jet in figure 8. Within the MLLA approach, these distributions vary in norm but not in shape, since the ratio $G(l,Y)/Q(l,Y)$ is fixed to the DLA value N_c/C_F. On the contrary, within the coherent branching formalism, the distributions in a quark jet and a gluon jet vary both in norm and shape. Figure 8 shows that in a wide preasymptotic range, $Y < 10$, say, adjusting Y and λ such that MLLA and the coherent branching formalism agree roughly for Q, the two formalisms will yield different curves for G. While there are marked differences in G/Q between both formalisms at all Y, for sufficiently large Y these differences die out in the region of large $l \sim \mathcal{O}(Y)$ to which the coherent branching formalism and the MLLA approach are tailored.

4 Identified parton distributions in quark and gluon jet

So far, we have discussed the distribution of *all* partons within a quark or a gluon jet. For related work on total parton multiplicities, we refer to [12,13]. The study presented in this section considers the more differential distributions of *quarks* and of *gluons* within a quark or a gluon jet. We characterize these distributions by subscripts. For instance, $Q^g(l,Y)$ is

JHEP05(2009)023

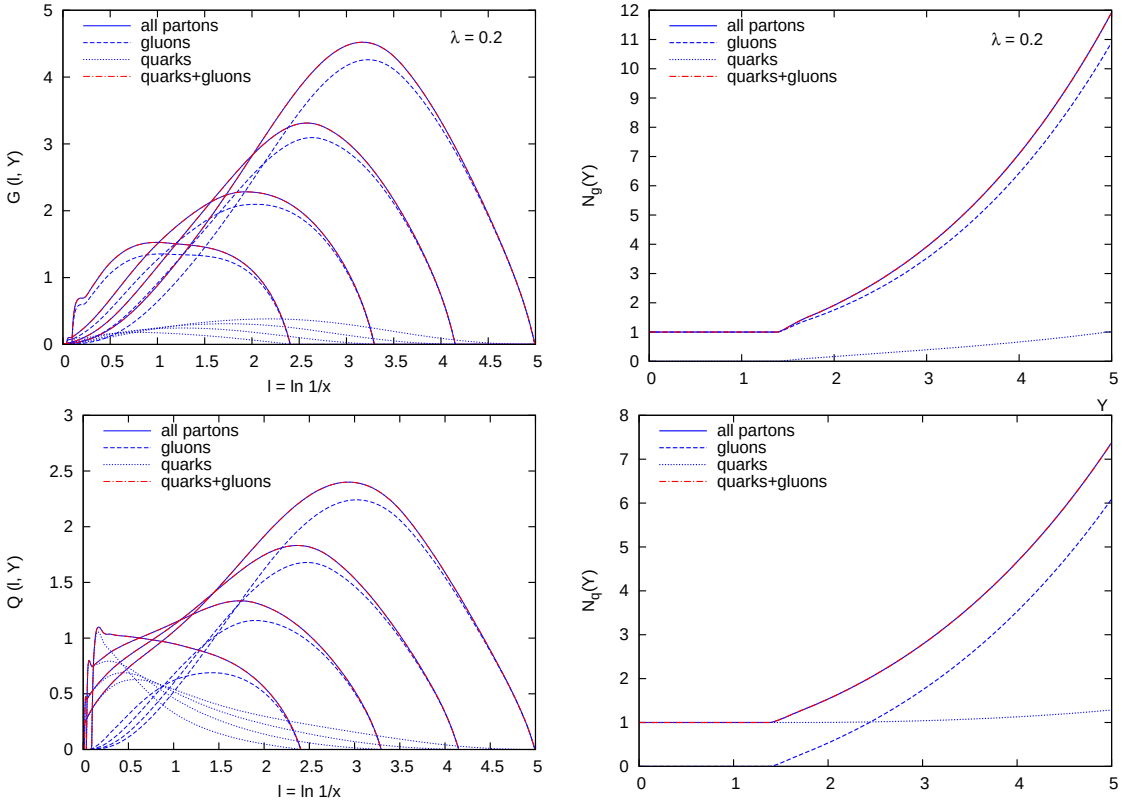

Figure 9. Left hand side: The continuous part of the single-parton distributions inside a gluon jet (upper panel) and a quark jet (lower panel). Different curves denote the single-quark (dashed) and single-gluon (dotted) distributions inside a jet, the explicit sum of these two distributions (dash-dotted), and its comparison to the distribution of all partons in a jet (solid) obtained by evolving the initial condition (2.10). The two latter curves coincide, as expected. Right hand side: the Y-dependence of the total multiplicity of quarks, gluons and all partons calculated for the cases shown on the left hand side.

the single-gluon distribution in a quark jet. As explained in subsection 2.1, single-quark distributions are obtained by evolving from the initial conditions (2.8) and single-gluon distributions are obtained by evolving from the initial condition (2.9). The phase space constraints imply that there is no evolution in the coherent branching formalism up to $Y = \ln 4$. Since the continuous parts of the distributions vanish by definition at $Y = \ln 4$, the initial conditions (2.8) and (2.9) translate directly to the initial conditions for the discrete parts

$$\begin{aligned} &\Delta_g(Y = \ln 4) = 0\,, \quad &&\Delta_q(Y = \ln 4) = 1\,, \quad &&\text{if only quarks are counted,} \\ &\Delta_g(Y = \ln 4) = 1\,, \quad &&\Delta_q(Y = \ln 4) = 0\,, \quad &&\text{if only gluons are counted.} \end{aligned} \tag{4.1}$$

It is straightforward to check that if a discrete part equals zero at $\ln 4$, then it stays zero at any value of Y.

In general, the distribution of quarks inside a jet is harder than that of gluons. This is a consequence of the fact that gluons are more likely to split. In the left panel of figure 9,

JHEP05(2009)023

which shows the identified parton spectra in jets for $\lambda = 0.2$, this is clearly seen for all values of Y. A particularly pronounced feature is seen in the single-quark distribution for quark jets: up to $Y = 5$, this distribution peaks at very large x values corresponding to $l < 0.5$. The integrated total quark multiplicity in this distribution, shown in the right panel of figure 9, remains of order unity during this evolution, indicating that this single quark distribution follows closely the momentum distribution of the evolved parent quark. This parent quark evolves via $q \to q\,g$ splittings predominantly by emitting soft gluons. For this reason, the quark distribution remains hard and the total multiplicity in the quark jet is largely dominated by subsequent $g \to g\,g$ splittings. It is in precisely this sense that the enhancement at large-x is a remnant of the δ-function in the initial condition, which gradually becomes negligible in the evolution to larger Y. For the distribution of quarks within a gluon jet, the situation is clearly different since the splitting function for $g \to q\,\bar{q}$ does not give rise to a logarithmic enhancement.

We have emphasized repeatedly that the approximations involved in deriving the coherent branching formalism do not guarantee an accurate description of the large-x region. We note, however, that the reasons which we have identified for the pronounced large-x enhancement of $Q^q(x, Y)$ in figure 9 do not refer to particular features of an $\mathcal{O}(\sqrt{\alpha_s})$ approximation, but emerge solely from generic features of the branching of quarks and gluons. As a consequence, we expect that these features, though observed outside the strict region of validity of the formalism explored here, correspond to physical reality and persist in a more complete formulation of the problem, which is accurate in the large-x region. Indeed, in Monte Carlo event generators, such an enhancement is seen on the level of partonic distributions [16–18]. In these event generators, it is generally the hadronization mechanism which connects the color of the leading quark to the rest of the event, and which thus leads to a hadronic single-inclusive distribution which is much softer than the partonic one.

For gluon jets as well as for quark jets, the jet multiplicity is ultimately dominated by gluons. The distribution of the hardest gluon in the first $g \to g\,g$ splitting process is likely to contribute significantly to the large values which $G(l, Y)$ shows in the large x region (say $l < 1.0$) for small values of Y. Upon further evolution in Y, this structure disappears faster in $G(l, Y)$ than in $Q(l, Y)$, since it is dominated in the first case by gluons, which split more readily than quarks.

5 Conclusion

We have calculated single parton distributions inside quark and gluon jets as a function of $\lambda = \ln Q_0/\Lambda_{\rm QCD}$ and $Y = \ln E/Q_0$ within the coherent branching formalism (2.3), and we have compared the results to those of the MLLA evolution equations (2.16) and (2.17). As discussed explicitly in section 2.2, the MLLA evolution equations can be obtained from the coherent branching formalism by a set of approximations, which are correct to next-to-leading order in $\sqrt{\alpha_s}$ within the kinematic range where $Y\,, l \sim \mathcal{O}(1/\sqrt{\alpha_s})$. Parametrically, both approaches are complete to the same order in $\sqrt{\alpha_s}$ within the same kinematical regime. However, there are significant qualitative differences.

JHEP05(2009)023

The coherent branching formalism conserves energy exactly, while the MLLA approach does not (see figure 5 and discussion in section 2.2). Moreover, while MLLA results approach a finite limiting spectrum for $\lambda \to 0$, this limit does not exist in the coherent branching formalism. In section 3.3, we have identified the approximations in deriving the MLLA approach, which are at the origin of this behavior. Of particular importance is an approximation of arguments of the coupling constant (approximation 2 in section 2.2), which is parametrically justified but which induces a qualitative difference in the solution if the regulator of the Landau pole is removed in the limit $\lambda \to 0$.

Although the differences between both formalisms arise at an order in $\sqrt{\alpha_s}$, at which both approaches are incomplete, we emphasize that these differences are worth studying on physical grounds. The MLLA ($\lambda \to 0$) limiting spectrum supplemented with LPHD is of particular physical interest since it provides a rather satisfactory description of a large body of experimental data with a minimal set of parameters. The coherent branching formalism is of particular interest, since (although not accurate to a higher order in $\sqrt{\alpha_s}$ than MLLA), it incorporates features which one may expect from a more complete treatment of higher-order terms. In particular, it supplements next-to-leading order accuracy in $\mathcal{O}(\sqrt{\alpha_s})$ with exact energy conservation. Moreover, it realizes a situation where in a perturbative calculation of single parton distributions, regularization of the Landau pole (i.e. finite λ) is needed to obtain a finite result. Thus, we have compared in the present work a phenomenologically successful approach with one, which is parametrically as accurate, but which incorporates additional physical features which may be expected from a more accurate treatment. This opens the opportunity to discuss the robustness of the physics conclusions of the phenomenologically successful approach in the light of a parametrically equally good and physically well-motivated different calculation.

The phenomenological success of the MLLA limiting spectrum supplemented by LPHD supports a picture, in which hadronization proceeds by perturbative evolution down to to the nominally non-perturbative scale $Q_0 = \Lambda_{\mathrm{QCD}}$, followed by a one-to-one mapping of partonic into hadronic distributions. The non-existence of the limit $Q_0 \to \Lambda_{\mathrm{QCD}}$ in another, parametrically equally accurate approach appears to question this picture. Here, we have shown that in the coherent branching formalism, where the $\lambda \to 0$-limit does not exist, single inclusive spectra within a quark or within a gluon jet can be made to matched rather well with a given MLLA limiting spectrum for small but finite $\lambda \sim 0.01$ and after slight adjustments of the hadronization scale and the normalization (which are fit parameters in phenomenological comparisons of MLLA). This is consistent with earlier observations that total jet multiplicities are best reproduced with fit values $\lambda \simeq 0.015 \pm 0.005$ [12], and that a satisfactory description of hadronic jet multiplicity moments can be obtained for $\lambda = 0.01$ [22]. On the other hand, the right hand side of figure 7 illustrates that the coherent branching formalism cannot be brought to agreement with the MLLA limiting spectrum for quark and gluon jets at the same time. Even if one allows for independent adjustments of the norm of Q and G, a visible difference in shape persists.

We close with some numerical estimates. The relation between the evolution variable Y and the jet energy E depends on the jet opening angle θ and the hadronization scale Q_0, as seen from eq. (2.1). In the case of large angles, the approximate formula (2.1) must

JHEP05(2009)023

be replaced by the exact relation $Y = \ln(E \sin\theta/Q_0)$. For a maximal jet opening angle $\theta = \pi/2$, we have then $E = \Lambda_{\rm QCD} \exp[Y + \lambda]$. Taking $\Lambda_{\rm QCD} = 200\,\text{MeV}$ and $\lambda \ll 1$, we find $E = 30\,\text{GeV}$ for $Y = 5$ and $E = 220\,\text{GeV}$ for $Y = 7$. The value $Y = 10$ corresponds to a jet energy $E > 4\,\text{TeV}$. So, for experimentally accessible jet energies, one should consider the range $5 < Y < 10$. We note that the above-mentioned differences between MLLA and the coherent branching formalism persist throughout the experimentally accessible Y-range.

Acknowledgments

We thank Yuri Dokshitzer, Wolfgang Ochs, Peter Richardson, Peter Skands, and Bryan Webber for helpful discussions at various stages during this work. We are particularly indebted to Krzysztof Golec-Biernat, who was a valuable discussion partner on all aspects of this study. S.S. is grateful to the CERN Theory Group for support and warm hospitality, and he acknowledges support from the Foundation for Polish Science (FNP) and a grant of the Polish Ministry of Science, N202 048 31/2647 (2006-08).

References

[1] Yu.L. Dokshitzer, V.A. Khoze, A.H. Mueller and S.I. Troyan, *Basics of perturbative QCD*, Frontierés, Gif-sur-Yvette France (1991).

[2] A.H. Mueller, *Multiplicity and hadron distributions in QCD jets: nonleading terms*, *Nucl. Phys.* **B 213** (1983) 85 [SPIRES].

[3] A.H. Mueller, *Square root of alpha (Q^2) corrections to particle multiplicity ratios in gluon and quark jets*, *Nucl. Phys.* **B 241** (1984) 141 [SPIRES].

[4] A. Bassetto, M. Ciafaloni and G. Marchesini, *Jet structure and infrared sensitive quantities in perturbative QCD*, *Phys. Rept.* **100** (1983) 201 [SPIRES].

[5] Y.L. Dokshitzer, V.A. Khoze, S.I. Troian and A.H. Mueller, *QCD coherence in high-energy reactions*, *Rev. Mod. Phys.* **60** (1988) 373 [SPIRES].

[6] C.P. Fong and B.R. Webber, *One and two particle distributions at small x in QCD jets*, *Nucl. Phys.* **B 355** (1991) 54 [SPIRES].

[7] I.M. Dremin and V.A. Nechitailo, *Average multiplicities in gluon and quark jets in higher order perturbative QCD*, *Mod. Phys. Lett.* **A 9** (1994) 1471 [hep-ex/9406002] [SPIRES].

[8] F. Arleo, R.P. Ramos and B. Machet, *Hadronic single inclusive kt distributions inside one jet beyond MLLA*, *Phys. Rev. Lett.* **100** (2008) 052002 [arXiv:0707.3391] [SPIRES].

[9] R. Perez-Ramos, F. Arleo and B. Machet, *Next-to-MLLA corrections to single inclusive $k_\perp$-distributions and 2-particle correlations in a jet*, *Phys. Rev.* **D 78** (2008) 014019 [arXiv:0712.2212] [SPIRES].

[10] I.M. Dremin and J.W. Gary, *Energy dependence of mean multiplicities in gluon and quark jets at the next-to-next-to-next-to-leading order*, *Phys. Lett.* **B 459** (1999) 341 [hep-ph/9905477] [SPIRES].

[11] A. Capella, I.M. Dremin, J.W. Gary, V.A. Nechitailo and J. Tran Thanh Van, *Evolution of average multiplicities of quark and gluon jets*, *Phys. Rev.* **D 61** (2000) 074009 [hep-ph/9910226] [SPIRES].

JHEP05(2009)023

[12] S. Lupia and W. Ochs, *Unified QCD description of hadron and jet multiplicities*, *Phys. Lett.* **B 418** (1998) 214 [hep-ph/9707393] [SPIRES].

[13] S. Lupia and W. Ochs, *Hadron multiplicity as the limit of jet multiplicity at high resolution*, *Nucl. Phys. Proc. Suppl.* **64** (1998) 74 [hep-ph/9709246] [SPIRES].

[14] Y.I. Azimov, Y.L. Dokshitzer, V.A. Khoze and S.I. Troyan, *Similarity of parton and hadron spectra in QCD jets*, *Z. Phys.* **C 27** (1985) 65 [SPIRES].

[15] Y.I. Azimov, Y.L. Dokshitzer, V.A. Khoze and S.I. Troyan, *Humpbacked QCD plateau in hadron spectra*, *Zeit. Phys.* **C 31** (1986) 213 [SPIRES].

[16] T. Sjöstrand, S. Mrenna and P. Skands, *PYTHIA 6.4 physics and manual*, *JHEP* **05** (2006) 026 [hep-ph/0603175] [SPIRES].

[17] G. Marchesini et al., *HERWIG: a Monte Carlo event generator for simulating hadron emission reactions with interfering gluons. Version 5.1 - April 1991*, *Comput. Phys. Commun.* **67** (1992) 465 [SPIRES].

[18] T. Gleisberg et al., *SHERPA 1.α, a proof-of-concept version*, *JHEP* **02** (2004) 056 [hep-ph/0311263] [SPIRES].

[19] R.P. Ramos, *Two particle correlations inside one jet at 'modified leading logarithmic approximation' of quantum chromodynamics. I: exact solution of the evolution equations at small x*, *JHEP* **06** (2006) 019 [hep-ph/0605083] [SPIRES].

[20] OPAL collaboration, M.Z. Akrawy et al., *A study of coherence of soft gluons in hadron jets*, *Phys. Lett.* **B 247** (1990) 617 [SPIRES].

[21] CDF collaboration, D.E. Acosta et al., *Momentum distribution of charged particles in jets in dijet events in $p\bar{p}$ collisions at $\sqrt{s} = 1.8$ TeV and comparisons to perturbative QCD predictions*, *Phys. Rev.* **D 68** (2003) 012003 [SPIRES].

[22] M.A. Buican, C. Förster and W. Ochs, *QCD explanation of oscillating hadron and jet multiplicity moments*, *Eur. Phys. J.* **C 31** (2003) 57 [hep-ph/0307234] [SPIRES].

JHEP05(2009)023